At the limit of total silane gas utilization for preparation of high-quality microcrystalline silicon solar cells at high-rate plasma deposition

A. Gordijn, A. Pollet-Villard, and F. Finger

Additional information on Appl. Phys. Lett.
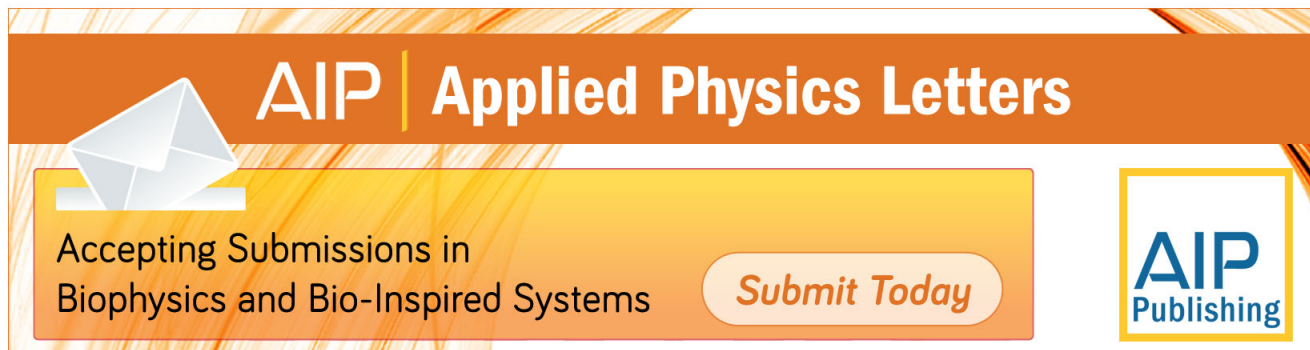
At the limit of total silane gas utilization for preparation of high-quality microcrystalline silicon solar cells at high-rate plasma deposition

A. Gordijn,[a)] A. Pollet-Villard, and F. Finger
IEK5-Photovoltaik, Forschungszentrum Jülich, D-52425 Jülich, Germany

It was aimed to find a regime for high-rate deposition of microcrystalline silicon with a silane gas utilization rate close to 100%. It is found that state-of-the art solar cells can be prepared at such conditions. The interdependencies of the relevant deposition parameters were identified in an experimental study in a multidimensional parameter space in which for each condition the μc-Si crystalline volume fraction was optimized to find the "optimum phase mixture." It is concluded that choice of the deposition pressure has a critical influence on the silane gas utilization rate and deposition rate. © *2011 American Institute of Physics*. [doi:10.1063/1.3593377]

Thin-film silicon solar cells based on hydrogenated microcrystalline silicon (μc-Si:H) bottom cells deposited by very-high frequency plasma-enhanced chemical vapor deposition (PECVD) were pioneered by Meier *et al.*[1] and are applied in solar module production, recently. Still, careful studies of the material and the growth process in order to increase the deposition rates and improve material quality are of utmost importance. Microcrystalline silicon is a mixed-phase material consisting of an amorphous phase, a crystalline phase, grain boundaries, and voids. The optoelectronic properties strongly depend on its crystallinity; μc-Si:H solar cells optimally perform at the "optimal phase mixture" of the μc-Si:H intrinsic absorber layer for which it is deposited in a regime that is close to the transition to the amorphous phase.[2–5] Generally, the material quality decreases with increasing deposition rate,[6] which is partly due to the high plasma power densities that involve a high-energy ion bombardment of the film during deposition. The application of high excitation frequencies[7] or high deposition pressures[8] or a combination of both[3] in PECVD is known to suppress the ion energy.

Investigation of the high deposition rate regime for μc-Si:H is of high relevance and several important aspects have already been identified. As the μc-Si:H properties strongly depend on the underlying layers, the most relevant and direct optimization procedure is to evaluate series of complete μc-Si:H-based p-i-n solar cells with varying i-layer properties.[3,4] An important precondition for the growth of μc-Si:H is the presence of atomic hydrogen.[9] High concentrations of atomic hydrogen occur at low silane concentrations (SC) of the source gas mixture from silane and hydrogen. The correlation between SC of the source gas, the degree of depletion of the silane gas (i.e., the fraction of silane that is decomposed by the plasma), and the amorphous-to-crystalline phase transition has been extensively studied by Strahm *et al.*[10] A high degree of silane gas depletion is found to promote the crystalline phase. Several studies point out that high discharge powers P, high deposition pressures p, a showerhead (SH) type of gas inlet through the powered electrode, and a small electrode distance are favorable for the high-rate deposition of high-quality μc-Si.[3,7,10–12]

In the present letter, the influences and the interdependencies of these individual processes and configuration parameters on the performance, deposition rate, and silane gas utilization rate of μc-Si:H solar cells (defined as the fraction of the silicon atoms entering the plasma as SiH_4 that contributes to the layer growth) are studied separately. Hereto, at each condition a series of complete solar cells with different source gas SC was made, leading to a variation in crystalline volume fraction in μc-Si:H. Thus, the point of "optimal phase mixture" can be identified for each series as the point leading to optimal solar cell performance. It is aimed to identify the crucial process parameters and find suitable process settings for the high-rate deposition of μc-Si:H at a silane gas utilization rate close to 100%.

Flat glass plates of 10×10 cm^2 covered with texture-etched ZnO:Al were used as substrates. Thereon, p-i-n solar cells were deposited with PECVD in the Cluster Tool that is described in Refs. 3 and 13. The B-doped μc-Si:H p-layers were grown at an excitation frequency of 94 MHz, and were optimized for light transmission, doping level, and crystallinity. Similar to Ref. 3, the μc-Si:H intrinsic absorber layers (i-layers) were deposited in a separate i-chamber at 94 MHz, using a mixture of silane (SiH_4) and hydrogen (H_2) as source gas [at a total gas flow F_t of 0.67 sccm/cm^2 (sccm denotes cubic centimeter per minute at STP), relative to the area of the powered electrode of $\sim$150 cm^2] and with a standard electrode distance d_e of 8 mm. An SH electrode was installed, whereby the possibility to admit the process gas from the side ["cross-flow" (CF) configuration, as applied in Ref. 3] was preserved. The n-layers were made of phosphorus-doped a-Si:H. Silver back contacts of 1 $\times$ 1 cm^2 were evaporated through a shadow mask. *J-V* characteristics of the test cells were measured under a simulated AM1.5 spectrum at 25 °C. The growth rates r_d were estimated from thickness measurements with a step profiler.

Figure 1 shows the efficiency and the open-circuit voltage as a function of SC for $P=0.13$ and 0.4 W/cm^2. The SiH_4 flow was varied to vary SC. Each series follow the general behavior that the open-circuit voltage V_{oc} gradually increases due to the decreasing crystalline phase. The efficiency η shows an optimum due to the optimum in the fill factor (FF) (not shown) and the continuous decrease in short-
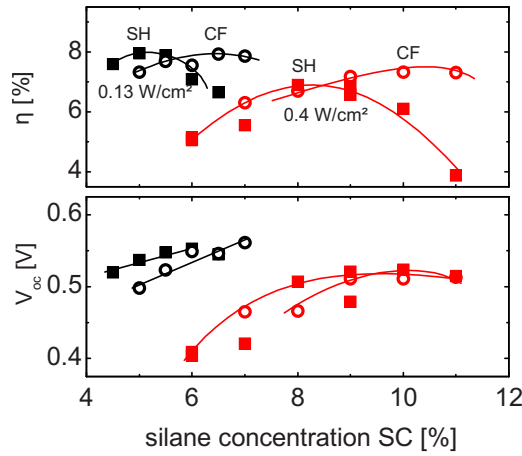
a)Electronic mail: a.gordijn@fz-juelich.de.

FIG. 1. (Color online) Efficiency and V_{oc} as a function of SC at p =2.1 mbar and P=0.13 and 0.4 W/cm^2 for SH configuration and CF configuration.
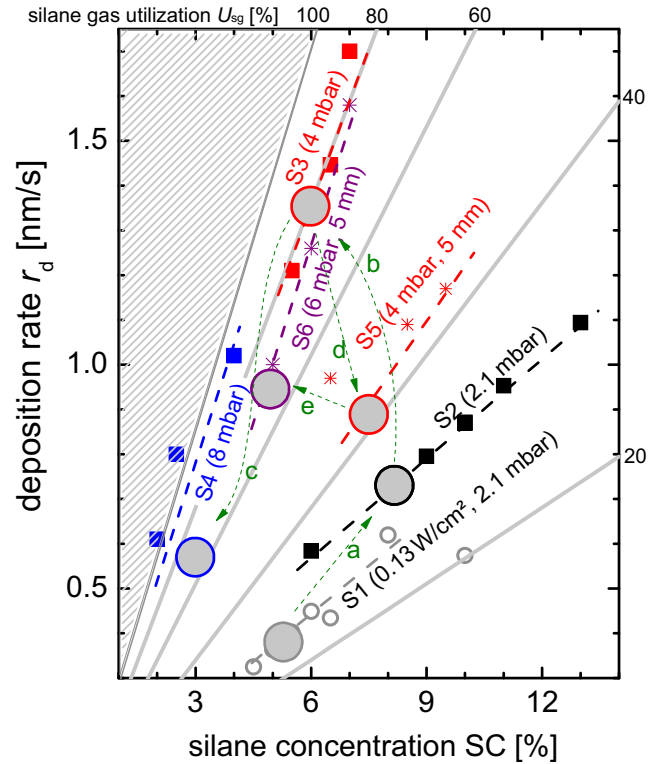

FIG. 2. (Color online) Deposition rate r_d as a function of SC for the different process conditions. If not stated otherwise P=0.4 W/cm^2 and d_e =8 mm for the series S1–S6. Data points within series are connected with color-coded dashed lines. For each series, the point of optimal solar cell performance is indicated with a large gray spot. The silane gas utilization rate U_{sg} is calculated for all SC and r_d based on Eq. (1) and visualized by gray solid lines. The line U_{sg}=100% represents the highest possible deposition rate based on the number of available silicon atoms.

circuit current density J_{sc} (not shown). A more detailed description and explanation of such behavior is given in Ref. 3.

SC$_{opt}$, defined as the SC at which the maximum solar cell efficiency η is reached, is higher for the CF configuration compared to SH. This is attributed to a higher availability of silane during the deposition due to the direct insertion of source gas into the plasma region. SC$_{opt}$ is also increasing with increasing P, which can be explained by the higher atomic hydrogen concentrations at higher P, as also described in Ref. 3. A high SC$_{opt}$ is an essential precondition for high-rate deposition because of the high availability of SiH$_4$.

At P=0.4 W/cm^2, using SH, the influences of deposition pressure p and electrode distance d_e were investigated in order to identify the effect on SC$_{opt}$, and the deposition rate at the optimum $r_{d,opt}$. At each condition a SC series of complete solar cells was made (similar to Fig. 1) in order to identify SC$_{opt}$. In Fig. 2, r_d and SC are plotted for these series. For each series, the point at SC$_{opt}$ is marked with a larger symbol. The series are labeled S1–S6 and the belonging deposition conditions can be found in Table I. The estimated silane gas utilization rates U_{sg} are indicated with gray solid lines. U_{sg} is defined as the ratio of the number of silicon atoms that is deposited on both electrodes over the number of silicon atoms that enters the reactor in the form of SiH$_4$ as follows:

$$U_{sg} = A r_d / F(\text{SiH}_4) n_{\text{Si}}, \quad (1)$$

where $F(\text{SiH}_4)$ is the silane flow into the reactor, n_{Si} the density of the growing film, and A the total deposition area, approximated as twice the area of the powered electrode. Nonuniformities of the film over the powered and grounded electrode lead to an error in U_{sg}. Note that the limit case of 100% silane gas utilization requires a silane gas depletion of 100% and the absence of powder formation in the gas phase.

It is observed that for each deposition condition, U_{sg} is more or less constant over the covered range of SCs. Note that even for the regime of S1, where $U_{sg} \sim 25\%$ only (in other words, there is plenty of Si atoms available in the plasma), r_d still strongly depends on the source gas flow of SiH$_4$. At higher SC, r_d is expected to saturate at the point where the power P will be rate limiting for the dissociation of SiH$_4$. The dependency of r_d on P in this regime is studied

by the effect of the increase in P from 0.13 to 0.40 mW/cm^2 for S1 and S2, respectively. Although P is tripled, r_d increases only by a factor smaller than 1.5 (arrow a). The upwards shift in SC$_{opt}$ with increasing P (as also observed in Fig. 1) leads to an effectively higher deposition rate $r_{d,opt}$ for the optimal solar cell material.

The effect of an increase in deposition pressure p from 2.1 to 8 mbar on $r_{d,opt}$ and SC$_{opt}$ can be considered by comparing S2, S3, and S4 (the closed symbols in Fig. 2). It is observed that with increasing p, SC$_{opt}$ continuously decreases (arrows b and c). Nevertheless $r_{d,opt}$ increases (arrow b) as a result of the increase in r_d for the whole series at 4 mbar (S3). In other words, the higher p facilitates the silane

TABLE I. Deposition parameters, r_d and photovoltaic parameters of the absorber layers of optimized solar cells of each series.

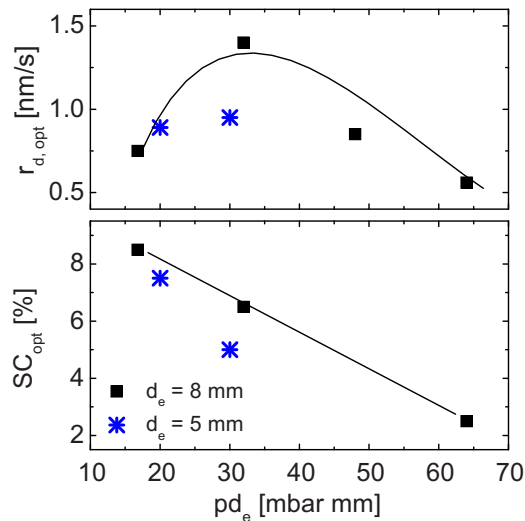| Series	S1	S2	S3	S4	S5	S6
P (W/cm^2)	0.13	0.40	0.40	0.40	0.40	0.40
p (mbar)	2.1	2.1	4	8	4	6
d_e (mm)	8 ± 1	8 ± 1	8 ± 1	8 ± 1	5 ± 1	5 ± 1
F_t (sccm/cm^2)	0.67	0.67	0.67	0.67	0.67	0.67
SC$_{opt}$ (%)	5.0	8.0	6.5	3.0	7.5	5.0
$r_{d,opt}$ (nm/s)	0.4	0.7	1.4	0.8	0.9	0.95
η (%)	8.0	6.9	7.4	7.4	6.2	8.1
V_{oc} (mV)	537	507	540	555	477	536
J_{sc} (mA/cm^2)	20.4	19.5	19.5	18.0	18.6	20.8
FF	73	70	70	74	70	72

FIG. 3. (Color online) SC_{opt} and $r_{d,opt}$ as a function of the product pd_e.

gas utilization for the optimal solar cell conditions. However, if U_{sg} reaches values of 80% or higher, a further increase in pressure is found to lead to a decrease in $r_{d,opt}$ (arrow c). This is a consequence of the reduced availability of SiH_4 source gas due to the observed decrease of SC_{opt} (arrow c) at this high pressure.

Following Paschen's law[14] very small electrode distances (<10 mm) are interesting for sustaining plasmas at very high pressures. On the other hand, their technical implementation is challenging, as only small geometrical deviations can lead to significant inhomogeneities in plasma properties. Starting from S3 ($p=4$ mbar), the effect of a decreased electrode distance d_e was studied. It was reduced from 8 to 5 mm for S5. In Fig. 2 it can be seen that the reduction in $r_{d,opt}$ and the slight increase in SC_{opt} (arrow d) follow the same trend as for a decrease in pressure (opposite direction of arrow b). From S5 ($p=4$ mbar; $d_e=5$ mm) an increase in p to 6 mbar was applied (S6) aiming to increase $r_{d,opt}$ by increasing U_{sg} (similar to arrow b for $d_e=8$ mm). It is shown that also at this d_e, an increase in p leads to a considerable increase in U_{sg} (arrow e). This leads to an increase in $r_{d,opt}$.

The effects of variations in d_e and p on $r_{d,opt}$ and SC_{opt} are plotted in Fig. 3 as a function of the product pd_e. This product is considered as an important characteristic of the plasma (Paschen's law) as it scales with the number of species that it contains. It is seen that the data for d_e of 5 and 8 mm are similar and follow the same trend, indicating that variations in p and d_e involve similar effects on U_{sg}.

All data in Figs. 2 and 3 were generated using the SH geometry. At high U_{sg}, it was observed that the CF geometry leads to considerably lower $r_{d,opt}$ and inhomogeneous deposition (not shown), which is considered to be a direct consequence of the inhomogeneous gas distribution.

In Table I, the photovoltaic parameters of the optimal solar cells of each series are listed. It should be noted that

here the solar cells serve as a characterization tool to indentified the optimal SC_{opt} for the optimum in efficiency for each series; they were not optimized for highest efficiencies. An initial efficiency of 7.4% was obtained at a high deposition rate $r_{d,opt}$ of 1.4 nm/s for S3 ($P=0.4$ W/cm^2, $p=4$ mbar, and $d_e=8$ mm). The absorber layer is 1 μm thick and the back contact is plain Ag. The best efficiencies for high deposition rates were obtained for S3 and S6 where U_{sg} is around 80% (see Fig. 2). This is considered to be the target value for U_{sg} for high-rate absorber layer deposition. To further increase r_d for optimized solar cells in this regime of high silane gas utilization, it is proposed to further increase the plasma power P and pressure p alternately for SC series of solar cells, analog to arrows a and b in Fig. 2.

In summary, it is found that an increase in p leads on the one side to an increase silane gas utilization rate U_{sg} and on the other side to a decrease in the SC_{opt} at which the optimum phase mixture occurs. These effects have opposite influences on the deposition rate at the optimum phase mixture $r_{d,opt}$. Therefore an optimum in $r_{d,opt}$ occurs at a certain pressure. It is concluded that state-of-the-art μc-Si:H based p-i-n solar cells can be made at a high silane gas utilization rate ($\sim$80%) at relatively high deposition rates (up to 1.4 nm/s).

[1] J. Meier, R. Flückiger, H. Keppner, and A. Shah, Appl. Phys. Lett. **65**, 860 (1994).
[2] O. Vetterl, F. Finger, R. Carius, P. Hapke, L. Houben, O. Kluth, A. Lambertz, A. Mück, B. Rech, and H. Wagner, Sol. Energy Mater. Sol. Cells **62**, 97 (2000).
[3] Y. Mai, S. Klein, R. Carius, J. Wolff, A. Lambertz, F. Finger, and X. Geng, J. Appl. Phys. **97**, 114913 (2005).
[4] G. Dingemans, M. N. van den Donker, A. Gordijn, W. M. M. Kessels, and M. C. M. van de Sanden, Appl. Phys. Lett. **91**, 161902 (2007).
[5] F. Finger, in *Thin-Film Silicon Solar Cells*, edited by A. Shah (EPFL, Lausanne, 2010), pp. 97–143.
[6] J. K. Rath, Sol. Energy Mater. Sol. Cells **76**, 431 (2003).
[7] F. Finger, P. Hapke, M. Luysberg, R. Carius, H. Wagner, and M. Scheib, Appl. Phys. Lett. **65**, 2588 (1994).
[8] L. Guo, M. Kondo, M. Fukawa, K. Saitoh, and A. Matsuda, Jpn. J. Appl. Phys. **37**, L1116 (1998).
[9] A. Matsuda, Thin Solid Films **337**, 1 (1999).
[10] B. Strahm, A. A. Howling, L. Sansonnens, and Ch. Hollenstein, Plasma Sources Sci. Technol. **16**, 80 (2007).
[11] A. Gordijn, J. K. Rath, and R. E. I. Schropp, Prog. Photovoltaics **14**, 305 (2006).
[12] M. Kondo, M. Fukawa, L. Guo, and A. Matsuda, J. Non-Cryst. Sol. **266**, 84 (2000).
[13] S. Klein, F. Finger, R. Carius, and M. Stutzmann, J. Appl. Phys. **98**, 024905 (2005).
[14] F. Paschen, Ann. Phys. **273**, 69 (1889).